

**Eucalyptus scab and shoot malformation: A
new disease in South Africa caused by a novel
species, *Elsinoe masingae***

**Jolanda Roux^{1,3*}, Michael J. Wingfield², Seonju Marincowitz³, Myriam Solís³,
Siphephelo Phungula¹ and Nam Q. Pham^{2, 2}**

¹Research Planning and Nurseries, Sappi Ltd, Howick, KwaZulu-Natal, 3290, South Africa

²Department of Plant and Soil Sciences, Forestry and Agricultural Biotechnology Institute (FABI), University of Pretoria, Pretoria, Gauteng, 0002, South Africa

³Department of Biochemistry, Genetics and Microbiology, Forestry and Agricultural Biotechnology Institute (FABI), University of Pretoria, Pretoria, Gauteng, 0002, South Africa

Corresponding author: Tel: +27 823293961; Email: jolanda.roux@sappi.com

A serious new disease of *Eucalyptus* was detected in South African plantations of these trees during the summer of 2021/2022. The first symptoms are minute dark spots on young leaves, petioles and shoots, becoming scab-like as the spots age. On highly susceptible *Eucalyptus* genotypes, leaves and shoots can become malformed leading to a “feathering” appearance in the tree canopies and in the case of heavy infections, leaf and shoot death occur. Isolations made directly from developing scabs resulted in slow-growing cultures. These were identified, based on phylogenetic analyses of DNA sequence data for the ITS, LSU, *TEF1* and *RPB2* regions, as a novel species of *Elsinoe* (Elsinoaceae, Myriangiales), described here as *E. masingae*. Inoculations on clonal plants of an *E. grandis* x *E. nitens* hybrid variety produced the same symptoms as those observed under natural conditions and the pathogen could be re-isolated from the emerging lesions. *Elsinoe masingae* is closely related to, but clearly distinct from the recently described *Elsinoe necatrix* that causes a serious scab and shoot malformation disease on *Eucalyptus* in Indonesia. Field surveys revealed significant variation in the susceptibility of different *Eucalyptus*

genotypes, with the most severely affected genotypes including an *Eucalyptus grandis* x *nitens* and an *E. grandis* x *urophylla* hybrid variety and *E. grandis*. The disease has also been observed on *Eucalyptus amplifolia* and on *E. dunnii*, which had very mild infections. The observed variation in susceptibility of *Eucalyptus* planting stock should provide opportunities to avoid serious damage due to scab caused by *E. masingae* in the future.

Introduction

Diseases caused by microbial pathogens represent one of the most important constraints to the sustainability of natural and planted forests globally (Wingfield *et al.*, 2015; Ramsfield *et al.*, 2016). More specifically, plantations of non-native species have been consistently and increasingly challenged by diseases (Wingfield *et al.*, 2008, 2015). Pathogens affecting industrial plantations include both native organisms that have found suitable hosts on the newly established tree species and pathogens that have been accidentally introduced into these non-native plantation environments (Branco *et al.*, 2015; Wingfield *et al.*, 2015). In the most serious of these cases, it can be necessary to change species or even the genera of trees being planted.

In South Africa, industrial plantations are comprised mostly of genotypes of the non-native genera *Acacia*, *Eucalyptus* and *Pinus* (Oberholzer, 2021), with *Eucalyptus* species and their hybrids representing approximately 44% of the commercially planted area in 2019. Sustainable production of these trees is, however, threatened by various factors, including insect pests and pathogens (Wingfield *et al.*, 2008; Roux *et al.*, 2012). In recent decades, pressures from pests and diseases have contributed significantly to changes in the plantation landscape, with a move away from pure species to planting hybrid combinations of different species (Morris, 2022). Deployment of pure *E. grandis*, for example, has largely been abandoned due to the impact of the canker pathogen *Chrysosporthe austroafricana* (Van Heerden *et al.*, 2005) and the gall wasp *Leptocybe invasa* (Dittrich-Schröder *et al.*, 2012).

The first *Eucalyptus* species were planted in South Africa in the early 19th century as garden trees. Large-scale commercial plantations of these trees were established in the latter half of the 19th century (Poynton, 1979). Initially these plantations were free of serious pests or pathogens, but over time this situation has changed. Pest and disease reports of *Eucalyptus* genotypes in South Africa have increased exponentially over the last 40 years. During the four decades prior to 1980, only three economically damaging diseases, Armillaria root rot (Kotze, 1935), Mycosphaerella leaf blotch (Doidge, 1950) and Phytophthora root rot (Wingfield and Knox-Davies, 1980), were recorded in South African plantations. However, in the subsequent period up to 2010, multiple additional diseases were recorded on *Eucalyptus* species (Roux *et al.*, 2012) and in the most recent decade up to 2023 two new diseases, Destructans leaf blight (Greyling *et al.*, 2016) and Ceratocystis wilt (Roux *et al.*, 2020) have been reported within five years of each other. This trend is likely to continue and requires intensified efforts to reduce the movement of infected plant material and the accidental introduction of new pests and pathogens as part of a global strategy (Wingfield *et al.*, 2015; Bonello *et al.*, 2022). This will require continuous monitoring and management of pests and diseases (Slippers *et al.*, 2020b) and must be aided by the application of precision pest management approaches (Slippers *et al.*, 2020a).

In late 2021 and early 2022, an unknown disease affecting the leaves and shoots of *Eucalyptus grandis* x *E. nitens* (GN) compartments was observed in the KwaZulu-Natal Province of South Africa.

Affected trees showed thinning of their canopies due to malformation of leaves. The aim of this study was to identify the cause of the disease based on isolations from the symptomatic tissues, analyses of DNA sequences of the resulting isolates and inoculations to investigate a causal relationship of the isolates. In addition, preliminary surveys were undertaken to determine the geographic extent of the disease and to gain a preliminary view of the likely long-term importance of the disease.

Methods

Disease symptoms and incidence

The newly observed disease was characterised by a thinning of the crowns of trees (~18 months-old), also described as a “feathering” of the branches (Figure 1A). These symptoms were first observed in late 2021 near Ixopo (30° 9'45.10"S 30° 0'15.99"E) in the KwaZulu-Natal Province of South Africa. The symptoms were initially thought to result from either environmental factors, nutrient imbalance, herbicide damage or damage by the snout beetle *Gonipterus* sp. 2. Closer inspection of trees showed that the symptoms were unlikely to be caused by an abiotic factor and the involvement of a biotic factor, other than *Gonipterus* sp. 2, seemed most likely.

Symptoms observed on diseased trees included undersized new leaves, often with reddish blemishes and/or small dark, sunken spots (Figure 1B, C, D). Raised spots, some with sunken black centres were also visible on young, green shoots (Figure 1E, G). On older leaves raised, scab-like spots were visible, sometimes accompanied by holes in the leaves (Figure 1A, E, F, G).

The first report of the disease was from a single plantation, with multiple compartments of the same variety (genotype) of *Eucalyptus* affected. This information was used to expand surveys for the disease, focusing on the known susceptible variety. Although a focus during the initial surveys was on the susceptible genotype, other genotypes were also inspected where they occurred in an affected area. A disease alert was also disseminated to all plantation managers, and reports of the disease were then investigated. Furthermore, observations of the disease were made during routine site visits to plantations in 2022, both in the KwaZulu-Natal as well as Mpumalanga Provinces of South Africa.

Microscopy and histopathology

Fresh leaves showing various stages of scab development were taken to a laboratory for detailed observation using microscopy. The leaves were examined under a dissection microscope (Nikon SMZ18, Japan) and images of lesions were captured using a camera (Nikon DS Ri2, Japan) mounted on a compound microscope (Nikon Eclipse Ni, Japan).

Colonisation of leaves was studied by preparing cross-sections through lesions using a cryostat microtome (Leica CM1520, Germany). Leaves containing scabs were cut into small pieces (about 5 × 5 mm) and mounted in a freezing medium (Leica, IL, USA). The mounted pieces were cut into 10–12 µm sections. The sections were mounted in 85% lactic acid and images captured with a camera mounted on a compound microscope (Nikon Eclipse Ni, Japan). Characteristic structures were measured using an imaging software program (Nikon NIS Elements-Br, Japan). The dimensions of the observed structures were presented as minimum – maximum (average ± standard deviation, n = number of measurements).



Figure 1 Typical symptoms of *Elsinoe masingae* infections on *Eucalyptus* in South Africa. (A) Infected trees with thinned canopies and shoot “feathering”, (B) small red spots developing brown/dead centres and eventually falling out of the leaf laminae to leave holes in the leaf surface, (C) small necrotic spots in young leaf, (D) necrotic black spot and older spot with developing scab, (E) typical scabs of older spots, with some spots starting to detach from leaf epidermis, (F) older scabs lifting from leaf surface as scab becomes dry, (G) older scabs lifting from leaf surface as scab becomes dry.

For Scanning Electron Microscopy (SEM), tissues containing lesions were cut into 1 × 1 mm pieces and placed in 2.5% glutaraldehyde/formaldehyde (50% v/v) for 24 h. The samples were then subjected to a dehydration process using a graded ethanol series at 30%, 50%, 70% and 90% for 15 min each, followed by four dehydration steps in 100% ethanol, three for 15 min each and 30 min for the final ethanol dehydration. Samples were placed onto plates containing hexamethyldisilazane (HMDS) and were subsequently mounted on aluminium stubs. The samples were coated with carbon using a Quorum Q150T Coating Unit (Quorum, United Kingdom) and visualised under a Zeiss 540 Gemini Ultra Plus FEG SEM (Zeiss, Germany) scanning electron microscope at the Laboratory for Microscopy and Microanalysis, University of Pretoria, Pretoria, South Africa.

Pathogen isolation and identification

Isolates

Samples of infected leaves and branches from the Ixopo region were collected in plastic zip-lock bags and kept cool until they could be stored in a refrigerator. Isolations were made as soon as possible after the samples had been collected. Leaf and branch material was surface disinfested using 70% ethanol and isolations made using a sterile hypodermic needle and a dissection microscope as described by Pham *et al.* (2021). Scabs were lifted from the leaves, petioles, shoots and branches and placed on either malt extract agar (MEA) containing 50g Neogen Malt Extract agar per litre of deionised water and amended with 0.05g/L streptomycin sulphate, or half-strength potato dextrose agar (PDA; BD Difco) in Petri dishes. Isolation plates were incubated for approximately one week at room temperature (~25°C) until hyphae began to grow from the infected tissues.

Pure cultures were established by transferring hyphal tips of the emerging fungi to fresh MEA plates. The isolated strains were deposited in the culture collection (CMW) of the Forestry and Agricultural Biotechnology Institute (FABI), University of Pretoria, South Africa. The holotype and ex-holotype specimens were deposited in the H.G.W.J. Schweickerdt Herbarium (PRU) and the culture collection (CMW-IA) of Innovation Africa at the University of Pretoria, South Africa.

DNA extraction, PCR amplification and sequencing

Prepman® Ultra Sample Preparation Reagent (Thermo Fisher Scientific, Waltham, MA, USA) was used to extract total genomic DNA from two-week-old isolates grown on PDA, following the manufacturer's protocols. The internal transcribed spacer regions 1 and 2 (ITS), including the 5.8S rRNA region, the nuclear large subunit (LSU) of the ribosomal RNA, a fragment of the DNA-directed RNA polymerase II second largest subunit (RPB2) and the translation elongation factor 1-alpha (TEF1) gene regions were amplified using the primers ITS1F and ITS4 (Gardes and Bruns, 1993; White *et al.*, 1990); LR0R and LR5 (Rehner and Samuels, 1994; Vilgalys and Hester, 1990), RPB2-5F and fRBP2-7cR (Liu *et al.*, 1999, Sung *et al.*, 2007) and elongation-1-F and elongation-1-R (Hyun *et al.* 2009) respectively.

The PCR reactions and conditions were the same as those used by Pham *et al.* (2019) and Fan *et al.* (2017). Amplified fragments of all loci were purified using ExoSAP-IT™ PCR Product Cleanup Reagent (Thermo Fisher Scientific, Waltham, MA, USA). Cleaned amplicons were sequenced in both directions using an ABI PRISM 3100 DNA sequencer (Thermo Fisher Scientific, Waltham, MA, USA) at the Sequencing Facility of the Faculty of Natural and Agricultural Sciences, University of Pretoria. Geneious Prime 2022.2.2 was used to assemble and edit the raw sequences (<https://www.geneious.com>). Sequences obtained in this study, for isolates from the Ixopo region, were deposited in GenBank (<http://www.ncbi.nlm.nih.gov>; Table 1).

Table 1. Collection details and GenBank accession numbers of species of *Elsinoe* obtained from this study and other species included in the phylogenetic analyses.

Species	Isolates ^a	Host	Locality	GenBank accession numbers ^b				References
				ITS	LSU	<i>RPB2</i>	<i>TEF1</i>	
<i>Elsinoe annonae</i>	CBS 228.64	<i>Annona</i> sp.	USA	KX887190	KX886954	KX887073	KX886836	Fan <i>et al.</i> (2017)
<i>E. caleae</i>	CBS 221.50 ^T	<i>Calea pinnatifida</i>	Brazil	KX887205	KX886968	KX887088	KX886851	Fan <i>et al.</i> (2017)
<i>E. centrolobii</i>	CBS 222.50 ^T	<i>Centrolobium robustum</i>	Brazil	KX887206	KX886969	KX887089	KX886852	Fan <i>et al.</i> (2017)
<i>E. citricola</i>	CPC 18535 ^T = RWB 1175	<i>Citrus limonia</i>	Brazil	KX887207	KX886970	KX887090	KX886853	Fan <i>et al.</i> (2017)
<i>E. diospyri</i>	CBS 223.50 ^T	<i>Diospyros kaki</i>	Brazil	KX887210	KX886973	KX887093	KX886856	Fan <i>et al.</i> (2017)
<i>E. eelemani</i>	DAR 83016 ^T	<i>Melaleuca alternifolia</i>	Australia	KX372292	N/A	KX398204	KX398203	Crous <i>et al.</i> (2016)
<i>E. erythrinae</i>	CPC 18530 = RWB 1138	<i>Erythrina</i> sp.	Brazil	KX887212	KX886975	KX887094	KX886858	Fan <i>et al.</i> (2017)
<i>E. eucalypticola</i>	CBS 124765 ^T = CPC 13318	<i>Eucalyptus</i> sp.	Australia	KX887215	KX886978	KX887097	KX886861	Fan <i>et al.</i> (2017)
<i>E. fagarae</i>	CBS 514.50 ^T	<i>Fagara riedelianum</i>	Brazil	KX887218	KX886981	KX887100	KX886864	Fan <i>et al.</i> (2017)
<i>E. fawcettii</i>	CBS 139.25 ^T	<i>Citrus</i> sp.	USA	KX887219	KX886982	KX887101	KX886865	Fan <i>et al.</i> (2017)
<i>E. fici</i>	CBS 515.50	<i>Ficus luschnathiana</i>	Brazil	KX887223	KX886986	KX887105	KX886869	Fan <i>et al.</i> (2017)
<i>E. fici-caricae</i>	CBS 473.62 ^T = ATCC 14652	<i>Ficus carica</i>	India	KX887224	KX886987	KX887106	KX886870	Fan <i>et al.</i> (2017)
<i>E. flacourtae</i>	CBS 474.62 ^T = ATCC 14654	<i>Flacourtia sepiaria</i>	India	KX887225	KX886988	KX887107	KX886871	Fan <i>et al.</i> (2017)
<i>E. ichnocarpi</i>	CBS 475.62 ^T = ATCC 14655	<i>Ichnocarpus frutescens</i>	India	KX887232	KX886995	KX887114	KX886878	Fan <i>et al.</i> (2017)

<i>E. jasmineae</i>	CBS 224.50 ^T	<i>Jasminum sambac</i>	Brazil	KX887233	KX886996	KX887115	KX886879	Fan <i>et al.</i> (2017)
<i>E. masingae</i>	CMW 58886	<i>Eucalyptus grandis</i> x <i>nitens</i>	Ixopo, South Africa	OQ678310	OQ678291	OQ676155	OQ676174	This study
<i>E. masingae</i>	CMW 58887	<i>Eucalyptus grandis</i> x <i>nitens</i>	Ixopo, South Africa	OQ678311	OQ678292	OQ676156	OQ676175	This study
<i>E. masingae</i>	CMW 58888^T = CMW-IA 1800	<i>Eucalyptus grandis</i> x <i>nitens</i>	Ixopo, South Africa	OQ678312	OQ678293	OQ676157	OQ676176	This study
<i>E. masingae</i>	CMW 58889	<i>Eucalyptus grandis</i> x <i>nitens</i>	Ixopo, South Africa	OQ678313	OQ678294	OQ676158	OQ676177	This study
<i>E. masingae</i>	CMW 58890	<i>Eucalyptus grandis</i> x <i>nitens</i>	Ixopo, South Africa	OQ678314	OQ678295	OQ676159	OQ676178	This study
<i>E. masingae</i>	CMW 58891	<i>Eucalyptus grandis</i> x <i>nitens</i>	Ixopo, South Africa	OQ678315	OQ678296	OQ676160	OQ676179	This study
<i>E. masingae</i>	CMW 58892	<i>Eucalyptus grandis</i> x <i>nitens</i>	Ixopo, South Africa	OQ678316	OQ678297	OQ676161	OQ676180	This study
<i>E. masingae</i>	CMW 58893	<i>Eucalyptus grandis</i> x <i>nitens</i>	Ixopo, South Africa	OQ678317	OQ678298	OQ676162	OQ676181	This study
<i>E. masingae</i>	CMW 58894 = CMW-IA 1801	<i>Eucalyptus grandis</i> x <i>nitens</i>	Ixopo, South Africa	OQ678318	OQ678299	OQ676163	OQ676182	This study
<i>E. masingae</i>	CMW 58895	<i>Eucalyptus grandis</i> x <i>nitens</i>	Ixopo, South Africa	OQ678319	OQ678300	OQ676164	OQ676183	This study
<i>E. masingae</i>	CMW 58896	<i>Eucalyptus grandis</i> x <i>nitens</i>	Ixopo, South Africa	OQ678320	OQ678301	OQ676165	OQ676184	This study

<i>E. masingae</i>	CMW 58897	<i>Eucalyptus grandis</i> x <i>nitens</i>	Ixopo, South Africa	OQ678321	OQ678302	OQ676166	OQ676185	This study
<i>E. masingae</i>	CMW 58898 = CMW-IA 1802	<i>Eucalyptus grandis</i> x <i>nitens</i>	Ixopo, South Africa	OQ678322	OQ678303	OQ676167	OQ676186	This study
<i>E. masingae</i>	CMW 58899	<i>Eucalyptus grandis</i> x <i>nitens</i>	Ixopo, South Africa	OQ678323	OQ678304	OQ676168	OQ676187	This study
<i>E. masingae</i>	CMW 58900	<i>Eucalyptus grandis</i> x <i>nitens</i>	Ixopo, South Africa	OQ678324	OQ678305	OQ676169	OQ676188	This study
<i>E. masingae</i>	CMW 58901	<i>Eucalyptus grandis</i> x <i>nitens</i>	Ixopo, South Africa	OQ678325	OQ678306	OQ676170	OQ676189	This study
<i>E. masingae</i>	CMW 58902 = CMW-IA 1803	<i>Eucalyptus grandis</i> x <i>nitens</i>	Ixopo, South Africa	OQ678326	OQ678307	OQ676171	OQ676190	This study
<i>E. masingae</i>	CMW 58903	<i>Eucalyptus dunnii</i>	Ixopo, South Africa	OQ678327	OQ678308	OQ676172	OQ676191	This study
<i>E. masingae</i>	CMW 58904	<i>Eucalyptus dunnii</i>	Ixopo, South Africa	OQ678328	OQ678309	OQ676173	OQ676192	This study
<i>E. necatrix</i>	CMW 56126	<i>Eucalyptus</i> sp.	Indonesia	MW079497	MW079515	MW086707	MW086721	Pham <i>et al.</i> (2021)
<i>E. necatrix</i>	CMW 56129 = CBS 147438	<i>Eucalyptus</i> sp.	Indonesia	MW079500	MW079518	MW086710	MW086724	Pham <i>et al.</i> (2021)
<i>E. necatrix</i>	CMW 56134 ^T = CBS 147439	<i>Eucalyptus</i> sp.	Indonesia	MW079505	MW079523	MW086715	MW086729	Pham <i>et al.</i> (2021)
<i>E. pitangae</i>	CBS 227.50 ^T	<i>Eugenia pitanga</i>	Brazil	KX887269	KX887032	KX887150	KX886914	Fan <i>et al.</i> (2017)

<i>E. populi</i>	CBS 289.64	<i>Populus deltoides</i> subsp. <i>deltoides</i>	Argentina	KX887273	KX887036	KX887154	KX886918	Fan <i>et al.</i> (2017)
<i>E. preissianae</i>	CBS 142129 ^T	<i>Eucalyptus preissiana</i>	Australia	KY173406	KY173498	N/A	N/A	Crous <i>et al.</i> (2016)
<i>E. randii</i>	CBS 170.38 ^T	<i>Carya</i> sp.	Brazil	KX887278	KX887041	KX887158	KX886923	Fan <i>et al.</i> (2017)
<i>E. tectiferae</i>	CBS 124777 ^T = CPC 14594	<i>Eucalyptus tectifera</i>	Australia	KX887292	KX887055	KX887172	KX886937	Fan <i>et al.</i> (2017)
<i>E. tiliae</i>	CBS 350.73 = ATCC 24510	<i>Tilia cordata</i>	New Zealand	KX887296	KX887059	KX887176	KX886940	Fan <i>et al.</i> (2017)
<i>E. verbenae</i>	CPC 18561 ^T = RWB 1232	<i>Verbena bonariensis</i>	Brazil	KX887298	KX887061	KX887178	KX886942	Fan <i>et al.</i> (2017)
<i>E. zizyphi</i>	CBS 378.62 ^T = ATCC 14656	<i>Zizyphus rugosa</i>	India	KX887303	KX887066	KX887183	KX886947	Fan <i>et al.</i> (2017)
<i>Myriangium hispanicum</i>	CBS 247.33	<i>Acer monspessulanum</i>	N/A	KX887304	KX887067	KX887184	KX886948	Fan <i>et al.</i> (2017)

^a ATCC = American Type Culture Collection, Virginia, USA; CBS = culture collection of Westerdijk Fungal Biodiversity Institute, Utrecht, the Netherlands; CMW = culture collection of the Forestry and Agricultural Biotechnology Institute (FABI), University of Pretoria, Pretoria, South Africa; CMW-IA = culture collection of Innovation Africa, University of Pretoria, Pretoria, South Africa; CPC = culture collection of Pedro Crous, housed at Westerdijk Fungal Biodiversity Institute; DAR = Plant Pathology Herbarium, New South Wales, Australia; RWB = personal collection of Robert Barreto.

^b ITS = internal transcribed spacer regions 1 and 2 including the 5.8S region of ribosomal RNA; LSU = nuclear large subunit (28S) of ribosomal RNA; *RPB2*: DNA-directed RNA polymerase II second largest subunit gene; *TEF1* = translation elongation factor 1- α gene.

^T Denotes ex-type strain.

N/A represents information that is not available.

Isolates obtained in this study are indicated in **bold**

Phylogenetic analyses

Reference sequences for species closely related to those emerging from this study were sourced from the GenBank database (Table 1). Alignments of all sequences were assembled using MAFFT v. 7 (<http://mafft.cbrc.jp/alignment/server/>) (Kato and Standley, 2013) and then confirmed manually in MEGA v. 7 (Kumar *et al.*, 2016). Maximum likelihood (ML) and Bayesian inference (BI) analyses were performed on data sets for each individual region and the four-locus concatenated data set. The most appropriate models were obtained using the software jModeltest v. 1.2.5. (Posada, 2008). ML analyses were conducted using RaxML v. 8.2.4 on the CIPRES Science Gateway v. 3.3 (Stamatakis, 2014) with a default GTR substitution matrix and 1,000 rapid bootstraps. BI analyses were performed using MrBayes v. 3.2.6 (Ronquist *et al.*, 2012) on the CIPRES Science Gateway v. 3.3. Four Markov Chain Monte Carlo (MCMC) chains were run from a random starting tree for five million generations, and trees were sampled every 100th generation. The first 25% of trees sampled were eliminated as burn-in, and the remaining trees were used to determine the posterior probabilities. Sequences for *Myriangium hispanicum* (CBS 247.33) were used as the outgroup in all phylogenetic analyses. Phylogenetic trees were viewed using MEGA v. 7 (Kumar *et al.*, 2016) and FigTree v. 1.4.4 (Rambaut, 2010).

Culture characteristics

Culture characteristics were studied on corn meal agar (CMA, Sigma-Aldrich, MO, USA), PDA and 2% MEA. Starter cultures were prepared by spreading mycelium onto half-strength PDA using a sterile needle. A mycelial plug (3 mm diam), collected from ten-day-old cultures, was placed at the centres of 65 mm Petri dishes containing each medium type. Five replicates of two strains (CMW 58888, CMW 58894) were incubated at temperatures ranging from 5–35 °C at 5-degree intervals in the dark for 30 d. When the growth study was terminated, the diameters of the colonies perpendicular to each other were measured and averages were used to calculate an approximate growth rate. Colour designations were made using Rayner's colour charts (Rayner 1970).

Pathogenicity tests

To confirm that the isolated fungus was the cause of the observed field symptoms, two isolates (CMW 58888, CMW 58894) were selected for inoculation onto plants of a *Eucalyptus grandis* x *E. nitens* (GN PP2107) variety in a phytotron at the University of Pretoria. The GN variety chosen for the trial was the same as that on which the disease was first observed under field conditions. Plants for inoculation were five-months-old and had been transplanted into 10 L bags in a composted bark medium. They were approximately 30 cm in height at the time of inoculation and had multiple young, newly developed shoots suitable for inoculation.

The fungal isolates were grown on half-strength PDA for three weeks at 22 °C. A mycelial suspension was prepared by adding sterile distilled water to the cultures and gently scraping the surface with a sterilised scalpel blade. The concentration of the mycelial fragment suspension was adjusted to approximately 10^6 mycelial fragments/ml with a haemocytometer and amended with one drop of Tween 20 (Sigma-Aldrich).

Six plants were inoculated per isolate by spraying the mycelial suspension on both upper and lower surfaces of the new shoots and the first two sets of expanded leaves until runoff. Six additional plants were sprayed with sterile distilled water and maintained as negative controls. The plants were enclosed in clear plastic bags together with paper towel soaked in distilled water to retain leaf wetness

and high humidity levels. Inoculated plants were maintained in a phytotron set at 25 °C under natural day-night light conditions.

Inoculated plants were monitored for the development of disease symptoms over a period of three weeks. Images of developing lesions were captured after seven days and again at the termination of the experiment. Inoculated leaves with necrotic spots were collected from each plant and surface-disinfested with 70% ethanol. Isolations were made from the spots as described previously. Resultant isolates were identified using DNA sequences of the ITS region.

Results

Disease incidence

The unknown disease considered in this study was first observed on young trees of the variety *E. grandis* x *E. nitens* (GN PP2107) in the Ixopo area of the KwaZulu-Natal Province. Surveys of similarly aged trees (6-18 months old) in this plantation showed that it was relatively wide-spread. In one compartment, stems of *E. dunnii* resprouting from stumps of the previous rotation also had symptoms of the disease. In this case, these were mild with small numbers of spots on some leaves.

Surveys undertaken in the subsequent six months confirmed the presence of the disease on variety GN PP2107 at multiple locations across the KwaZulu-Natal Province. The disease was also found on pure *E. grandis* trees in two trials and on *E. grandis* x *E. urophylla* varieties in the KwaZulu-Natal and Mpumalanga Provinces (Figure 2) as well as on *E. amplifolia* planted in a research trial near Richmond in KwaZulu-Natal.

Considerable variation in symptom incidence and severity was observed between compartments and on different *Eucalyptus* genotypes. This variation in symptom development was also found on trees in the same compartment and sometimes on the same tree. The disease appeared more severe in areas with higher moisture and on the sides of trees that remained wetter for longer periods of the day.

Infection and symptom development

Infection was initiated with the degradation of the leaf cuticle after which the pathogen grew into the epidermal cells (Figure 3A). The infected epidermal cells lost their viability, collapsed, were intermingled with fungal hyphae, and became unrecognisable (Figure 3B). Cells adjoining the infected cells began to display a hardening of the cell walls (Figure 3B). A similar process of disease development was observed as the causal agent colonised the mesophyll cells (Figure 3C, D). When colonisation progressed from the adaxial to abaxial surface or *vice versa*, the adjoining cells of the colonised lesions became lignified, resulting in the lesions detaching from the healthy cells to produce scab-like structures. Scab-like lesions and eroding of the leaf cuticle could be clearly seen using SEM (Figure 4A). Fungal fruiting structures producing conidia were infrequently observed, developing within the epidermal cells and becoming erumpent (Figure 3 E-I; Figure 4B-D).

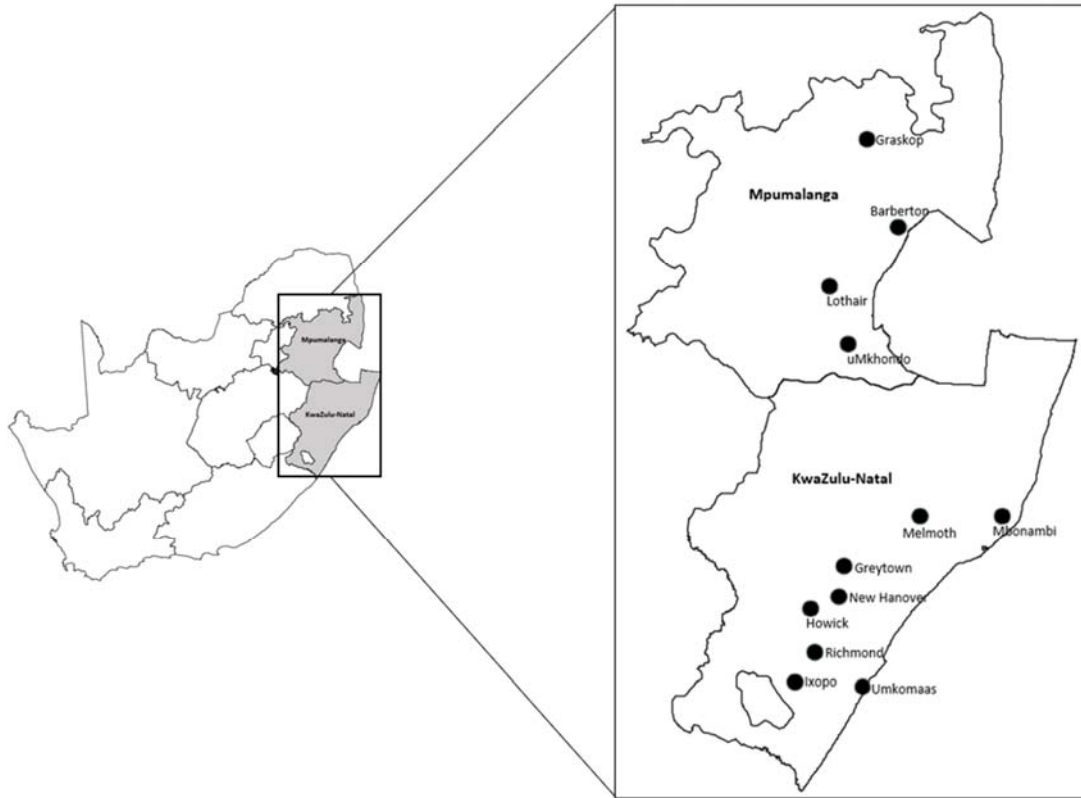


Figure 2 Map showing the current known distribution of the scab disease caused by *Elsinoe masingae* on *Eucalyptus* in South Africa (names indicate closest town/city to affected plantations).

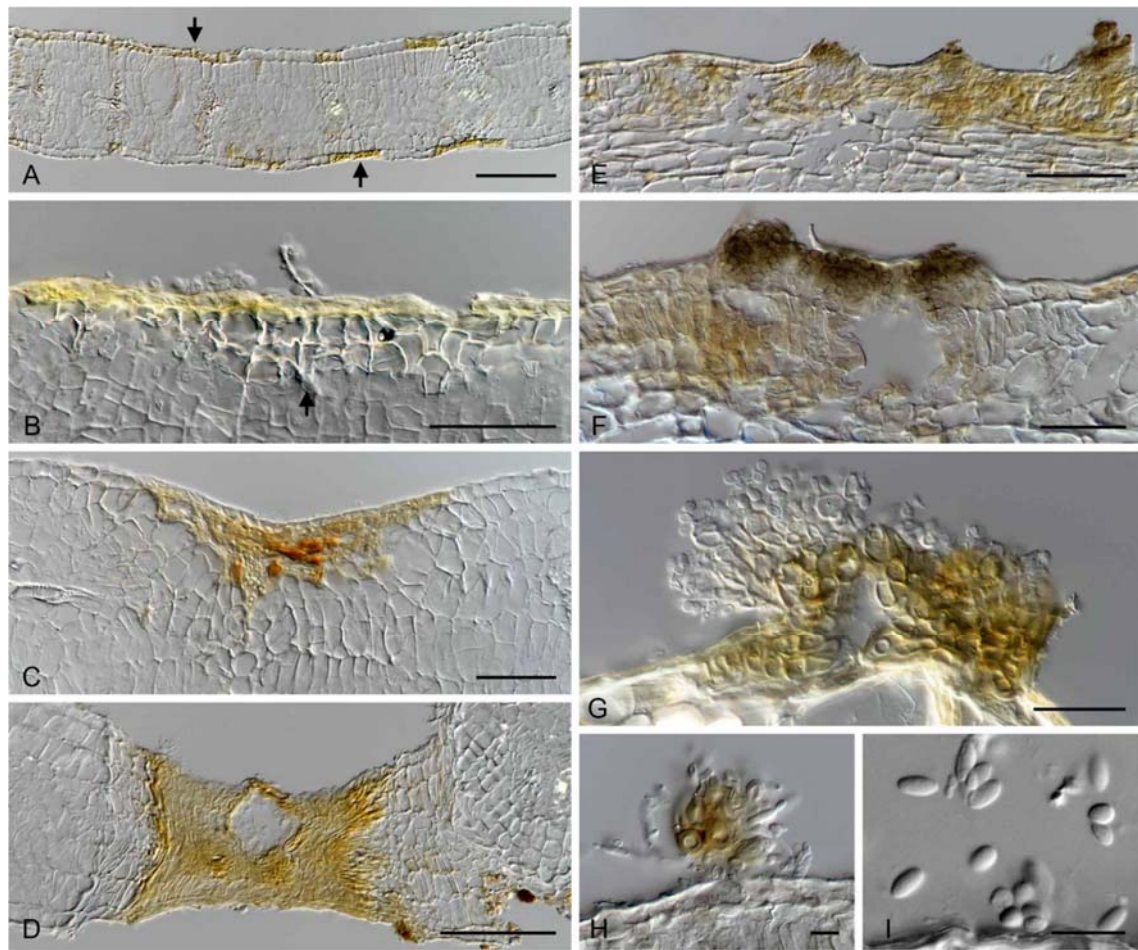


Figure 3 Colonisation of *Eucalyptus* leaf tissue by *Elsinoe masingae*. (A) Epidermal cells occupied by the fungal hyphae (arrows), (B) collapsed epidermal cell and its adjoining cells of which cell walls were hardened and lost viability, (C) advancement of the fungus beyond epidermal cells, (D) complete colonisation of the fungus from the adaxial to abaxial surface and collapsing adjoining cells, (E, F) conidiomata formed within the epidermal cells and became erumpent, (G, H) close-up of conidioma with conidiogenous cells, (I) conidia. Scale bars: A, E = 100 µm; B–D, F = 50 µm; G = 25 µm; H, I = 10 µm.

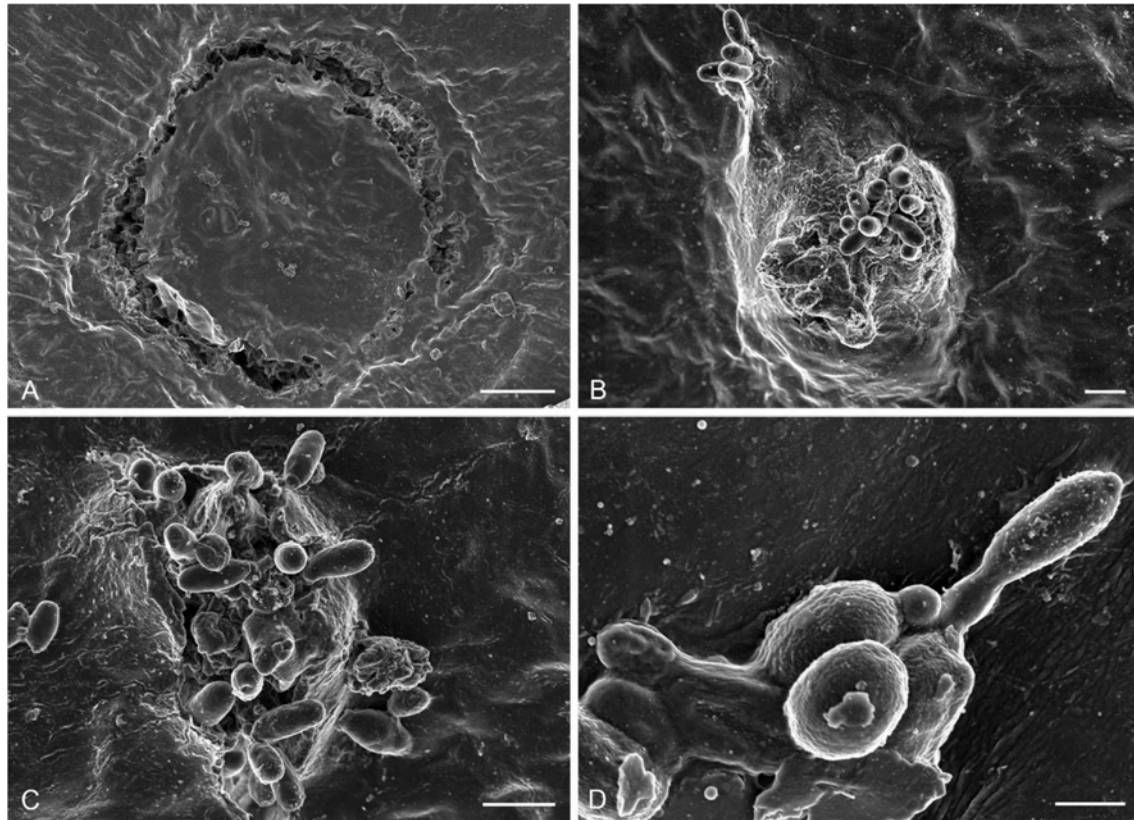


Figure 4 Scanning electron micrograph of *Elsinoe masingae* on *Eucalyptus grandis* x *nitens* leaves. (A) Separation of the infected lesion (necrotic spot) from the non-infected tissue, (B, C) erumpent fruiting structures, (D) conidium attached to a conidiogenous cell, showing its holoblastic conidiogenesis. Scale bars: A = 50 μm ; B, C = 5 μm ; D = 2 μm .

Pathogen isolation and identification

Isolations

Isolations from scab-like spots on leaves, petioles and shoots resulted in slow-growing cultures of similar morphology. A total of 19 isolates were obtained from the material collected at Ixopo. Of these, 17 were from *E. grandis* x *nitens* and two were from *E. dunnii*.

Phylogenetic analyses

Sequence data were generated for all 19 isolates and were approximately 550 bp for the ITS region, 890 bp for the LSU, 900 bp for the *RBP2* and 390 bp for the *TEF1*. Blast searches (NCBI Genbank) showed that these isolates belonged to the genus *Elsinoe*, with the highest sequence similarity to *E. necatrix*. *Elsinoe* species included in the phylogenetic analyses were those that were most closely related to the *Eucalyptus* isolates from South Africa and within the same larger phylogenetic clade for the genus *Elsinoe* (Fan *et al.* 2017; Marin-Felix *et al.*, 2019). For the phylogenetic analyses of each individual data set, the HKY+I model was selected for ITS and the GTR+I model for LSU, *RBP2* and *TEF1*. ML trees for each individual gene region with bootstrap support values of ML and posterior probabilities of BI were constructed (Figure S1). The topologies of the single gene phylogenies were

ITS+LSU+RPB2+TEF1



Elsinoe masingae sp. nov.

Figure 5 Phylogenetic tree based on maximum likelihood (ML) analysis of a concatenated DNA data set of ITS, LSU, *RPB2*, and *TEF1* sequences for *Elsinoe* species. Bootstrap values $\geq 70\%$ for ML analyses and posterior probabilities values ≥ 0.9 obtained from Bayesian inference (BI) are indicated at the nodes as ML/BI. Bootstrap values $< 70\%$ or probabilities values < 0.9 are marked with “*”, and nodes lacking the support values are marked with “-”. Isolates representing ex-type material are marked with “T”. *Myriangium hispanicum* (isolate CBS 247.33) represents the outgroup.

similar and largely adhered to the Genealogical Concordance Phylogenetic Species Recognition (GCPSR) concept (Taylor *et al.* 2000).

The combined sequence data set used in the phylogenetic analyses included 45 ingroup taxa and 2408 characters, including alignment gaps. Topologies of the trees resulting from the ML and BI analyses were concordant and showed similar phylogenetic relationships between taxa (Figure 5). The nineteen isolates from *Eucalyptus* in South Africa considered in this study had identical sequences and formed a well-supported (ML/BI = 100/1.00) monophyletic clade in the phylogenetic tree (Figure 5), clearly distinct from the most closely related species, *E. necatrix*, based on the GCPSR concept and thus represent a novel taxon.

Taxonomy

Elsinoe masingae Jol. Roux, N.Q. Pham, Marinc. & M.J. Wingf. **sp. nov.** Figs. 3, 4

MycoBank: MB 848229

Etymology: Named for Mr Sandile Masinga, an enthusiastic South African forester who's sharp observational skills and determination to identify the cause of an unknown malady of trees under his management led to the first confirmed report of the new *Eucalyptus* scab disease described in this study.

Diagnosis: Similar to *E. necatrix* but differs in having a slower growth rate on PDA. It can be differentiated from *E. necatrix* by ITS (6 bp), LSU (1 bp), *RPB2* (8 bp) and *TEF1* (9 BP) sequences.

Typification: South Africa: Kwa-Zulu Natal Province, Ixopo, Sutton Plantation. Symptomatic leaves of *Eucalyptus grandis* × *E. nitens*. 29 April 2022. Jolanda Roux. [Holotype PRU(M) 4525; ex-holotype culture CMW-IA 1800, CMW 588880]. GenBank: OQ678312 (ITS); OQ678293 (LSU); OQ676157 (*TEF1*); OQ676176 (*RPB2*).

Description: **Sexual morph** not observed. **Asexual morph** on substrate, rarely encountered. **Conidiomata** acervular, solitary or closely aggregated, dark brown, epidermal, initially immersed, later becoming erumpent, composed of thick-walled, pale brown to brown pseudoparenchyma, textura angularis, 131–376 × 67–189 µm (195.5 ± 69.23 × 97.2 ± 39.75 µm, n = 10). **Conidiophores** borne on pseudoparenchyma, hyaline to pale brown. **Conidiogenous cells** phialidic, hyaline, ampulliform to lageniform. **Conidia** hyaline, oval, aseptate, 3–5 × 1.5–3 µm (4.2 ± 0.44 × 1.8 ± 0.29 µm, n = 45).

Culture characteristics: **Colonies on PDA, CMA, MEA** at all temperatures showing circular growth with uneven edges, flat (CMA) or raised with radial grooves or cerebriform (PDA, MEA), mycelia mostly immersed having a shiny (CMA) or velvety appearance with short aerial hyphae (PDA, MEA), medium dense (CMA) or densely compact (PDA, MEA), a few colonies at 20–30 °C (MEA), 30 °C (PDA), 25 and 30 °C (CMA) secreting scarlet (7i) pigment on media. Colour **on PDA** above mixed patches of saffron (13f), ochreous (13'b), fulvous (11'i) to umber (13'k) (10–25 °C), orange (13b), sienna (13l) to blood colour (1m) (30°C), reverse fulvous (13'i), rust (7'k) to chestnut (7'm). Colour **on CMA** above sienna (13i) (10–25 °C), chestnut (7'm) (30 °C) patches on ochreous (13'b) background, reverse rust (7'i) (10–25 °C), chestnut (7'm) (30 °C) patches on ochreous (13'b) and umber (13m) background. Colour **on MEA** above patches or sectors of chestnut (7'm) or blood colour (1m) mixed with orange (13b) or ochreous (13'b), sienna (13i), reverse chestnut (7'm). Optimum growth temperature at 25 °C reaching 16.3 (PDA), 11.9 (CMA), 22 (MEA) mm diam in 30 d, growth limited to mycelial plug at 5 °C, no growth and irreversible damage at 35 °C (Figure 6).

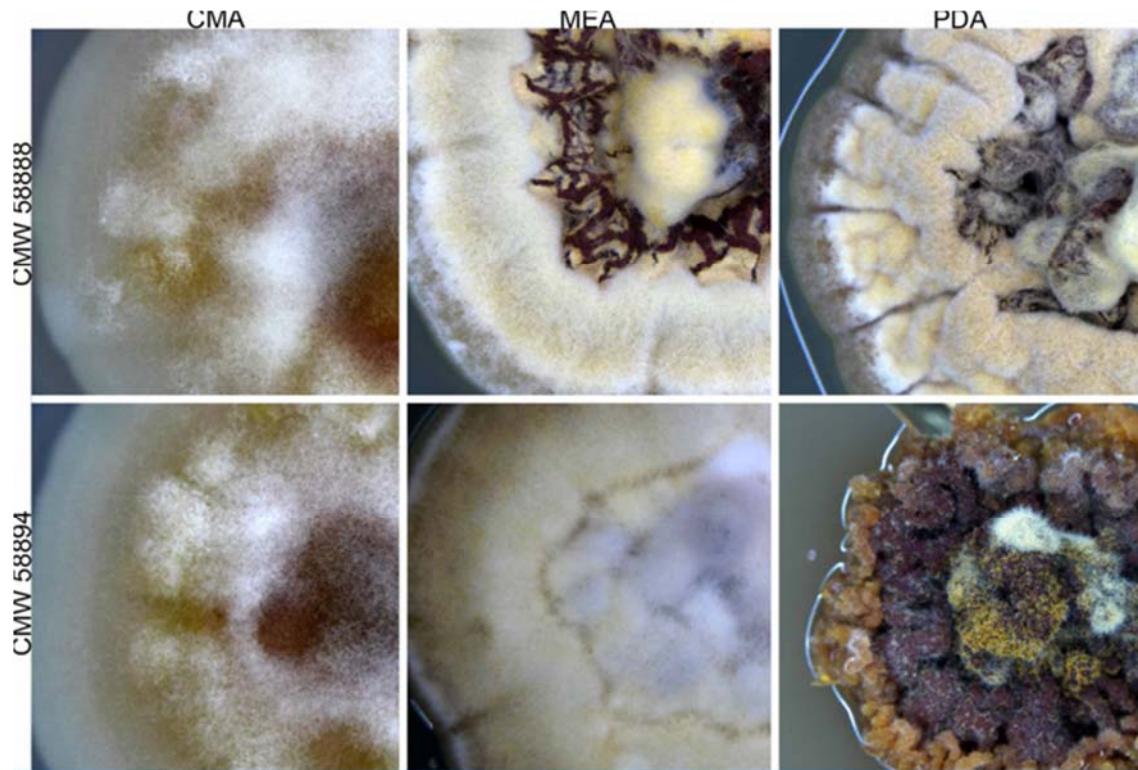


Figure 6 Culture morphology of *Elsinoe masingae* isolates CMW 58888 = CMW-IA 1800 (ex-holotype) and CMW 58894 = CMW-IA 1801 incubated in the dark for 31 d on CMA, 2% MEA and PDA.

Habitat: Associated with scab and malformation of leaves and shoots of *Eucalyptus* species.

Known distribution: South Africa (Kwa-Zulu Natal, Mpumalanga)

Other material examined: South Africa: Kwa-Zulu Natal Province, Ixopo, Sutton plantation. *Eucalyptus grandis* × *nitens*. 29 April 2022. Jolanda Roux. [PRU(M) 4526; culture CMW-IA 1801, CMW 58894]. GenBank: OQ678318 (ITS); OQ678299 (LSU); OQ676163 (*RPB2*); OQ676182 (*TEF1*); [PRU(M) 4527; culture CMW-IA 1802, CMW 58898]. GenBank: OQ678322 (ITS); OQ678303 (LSU); OQ676167 (*RPB2*); OQ676186 (*TEF1*); [PRU(M) 4528; culture CMW-IA 1803, CMW 58902]. GenBank: OQ678326 (ITS); OQ678307 (LSU); OQ676171 (*RPB2*); OQ676190 (*TEF1*).

Notes: *Elsinoe masingae* showed a close affinity to *E. necatrix*, *E. eucalypticola* and *E. eelemani* in the phylogenetic analyses. No conidial dimensions have been published for *E. necatrix*, which was described based only on DNA sequence data and culture morphology (Pham *et al.* 2021). *Elsinoe masingae* (3–5 × 1.5–3 μm) can be distinguished from *E. eelemani*, which has larger conidia (4.5–8 × 2–3.5 μm) and which is known from tea trees (*Melaleuca alternifolia*) in Australia (Crous *et al.* 2016). *Elsinoe eucalypticola* is known based on the characteristics of its sexual state (Cheewangkoon *et al.*, 2009). Both *E. masingae* and *E. eucalypticola* share the same optimum growth temperature (25 °C) on MEA, but the former species grows more rapidly (0.32 mm/d) than the latter species (0.20 mm/d). *Elsinoe necatrix* is the most closely related species to *E. masingae* and both species grow optimally on PDA at 25 °C, but the former species grows more rapidly (0.28 mm/d) than the latter species (0.21 mm/d).

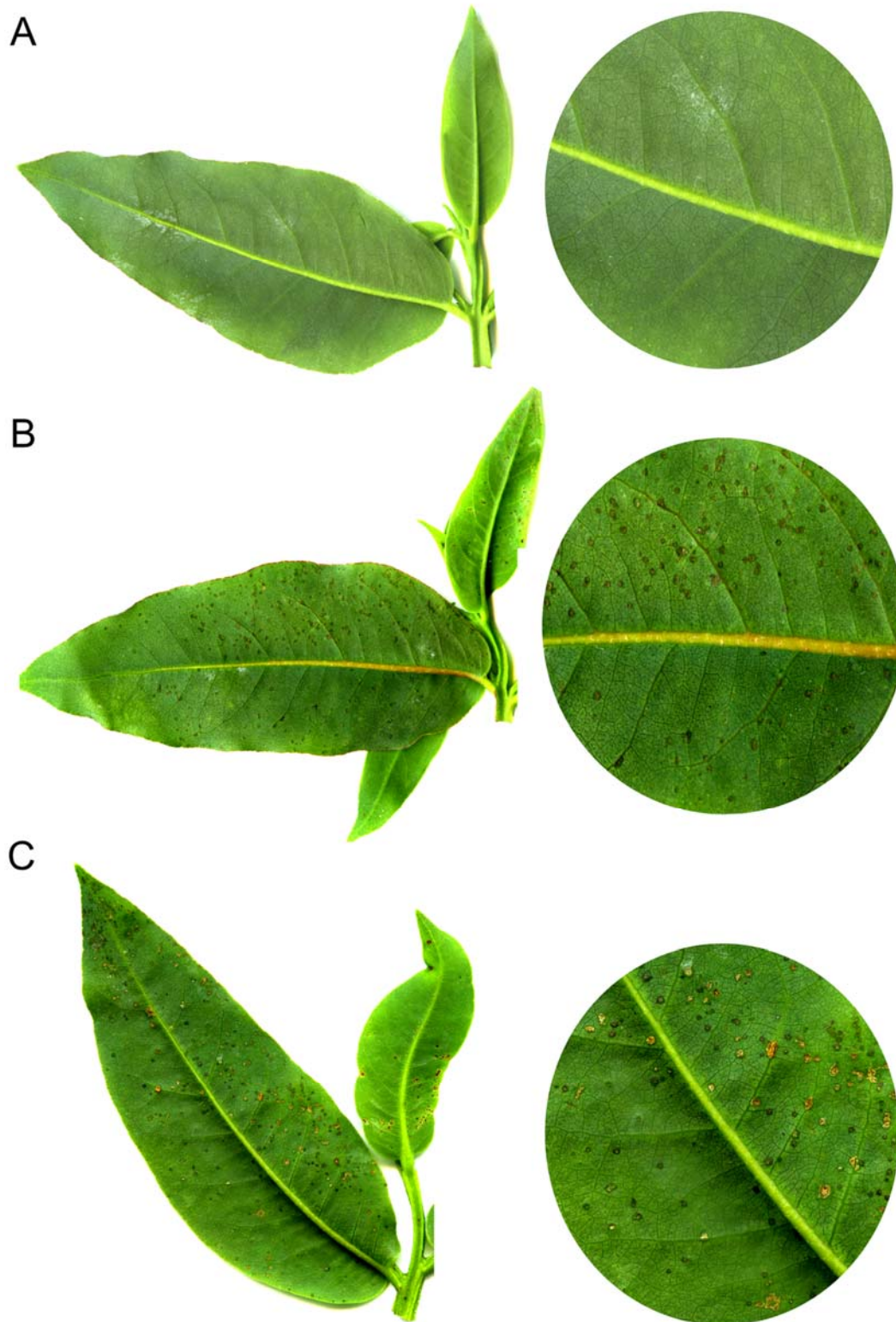


Figure 7 Results of inoculation with *Elsinoe masingae*. (A) Control, (B, C) Necrotic spots developed after seven and eighteen days (B: CMW 58888 = CMW-IA 1800, C: CMW 58894 = CMW-IA 1801).

Pathogenicity tests

Minute dark spots became visible on the young leaves of inoculated plants within three days after inoculation. Additional spots developed during the course of the next few days and after seven days all inoculated plants showed the presence of spots on young leaves similar to those observed under field conditions (Figure 7A). The experiment was terminated after two and a half weeks, as by that time scab-like spots had developed on inoculated leaves (Figure 7B). For some plants, holes had become visible in the leaves (Figure 7C). No symptoms were observed on the plants inoculated as controls (Figure 7D).

Isolations were made from scab-like lesions resulting from the inoculations on half-strength PDA. The resultant isolates were identified as *E. masingae* based on their ITS sequences. Re-isolation of the inoculated fungus from symptoms typical of those observed under field conditions satisfied the requirements of Koch's Postulates and confirmed that *E. masingae* is the causal agent of the scab disease on *Eucalyptus* genotypes in South African plantations.

Discussion

The present study reports the presence of a new leaf and shoot disease of *Eucalyptus* that has recently appeared in South Africa. The symptoms are typical of scab diseases caused by species of fungi in the genus *Elsinoe*. The causal agent was identified based on DNA sequence comparisons of four regions (ITS, LSU, *RPB2* and *TEF1*) as a novel species described here as *E. masingae*. The pathogenicity of the fungus was confirmed in an inoculation trial utilising the same variety of *Eucalyptus* on which the disease was first found under field conditions.

While scab diseases caused by species of *Elsinoe* are known on a number of crop plants (Fan *et al.*, 2017; Marin-Felix *et al.*, 2019; Li *et al.*, 2021), these were not known on *Eucalyptus* until recently. This situation changed when a scab disease similar to the one described in this study emerged in *Eucalyptus* plantations in north Sumatra and for which the causal agent was described as *E. necatrix* (Pham *et al.*, 2021). The *Eucalyptus* scab disease described in this study, and caused by a new species of *Elsinoe*, is thus only the second to have emerged on this host. It suggests that this category of disease may be emerging as important constraints to *Eucalyptus* forestry in the future.

Eight species of *Elsinoe* namely *E. eucalypti*, *E. eucalypticola*, *E. eucalyptigena*, *E. eucalyptorum*, *E. eucalypticola*, *E. preissianae*, *E. tectiferae* and *E. necatrix* have been described from *Eucalyptus* species (Crous *et al.*, 2019; Marin-Felix *et al.*, 2019; Pham *et al.*, 2021). With the exception of *E. necatrix*, all of these species have been described from Australia (Summerell *et al.*, 2006; Cheewangkoon *et al.*, 2009; Crous *et al.*, 2016, 2019; Fan *et al.*, 2017; Marin-Felix *et al.* 2019). Other than *E. masingae* described in the present study, *E. necatrix* is the only species known to cause a serious disease and for which pathogenicity has been tested experimentally. It is possible that the other *Elsinoe* species on *Eucalyptus* are primary pathogens and suggests that *E. necatrix* and *E. masingae* could have an origin in areas where *Eucalyptus* is native. It is also possible that these *Elsinoe* species have originated via a host jump from other native trees in the Myrtaceae. This is credible as a number of *Elsinoe* species have been described from other hosts in the Myrtaceae, including *Eugenia*, *Lophostemon* and *Melaleuca* (Crous *et al.*, 2016; Fan *et al.*, 2017) and in phylogenetic analyses *E. masingae* groups in a larger sub-clade containing *E. eelemani* from *Melaleuca alternifolia*. Both hypotheses should be tested and population genetic studies on *E. masingae* will be initiated to obtain an indication of its possible origin.

Disease symptoms and the histopathology of pathogen development observed on *Eucalyptus* plants infected with *E. masingae* are similar to those caused by *E. necatrix* on *Eucalyptus* in Indonesia (Pham *et al.*, 2021). Of all the symptoms, the scab-like spots that are released from the mesophyll tissues resulting in holes in the leaves are the most definitive. Likewise, the so-called “feathering” of the young shoots are typical of both diseases and are thought to arise from a toxin being produced by the pathogens. This would be consistent with the fact that those *Elsinoe* species known to cause disease produce the toxin Elsinochrome that is important in disease development (Liao and Chung, 2008; Li *et al.*, 2021).

Scab and leaf malformation caused by *E. masingae* is already relatively wide-spread in *Eucalyptus* plantations in South Africa. During surveys conducted in 2022, it was confirmed from two of the major *Eucalyptus* growing regions in the country, namely the KwaZulu-Natal and Mpumalanga Provinces. It is likely that the disease has been present in the country for several years but was not recognised due to the unusual disease symptoms and the difficulty in isolating the pathogen (Pham *et al.*, 2021). Corky spots and small holes in leaves have been observed on *Eucalyptus* leaves for several years, but at much lower incidence and in the absence of the severe disease symptoms seen in 2021 and 2022. The increased incidence and severity of the disease are likely associated with the higher than average rainfall experienced in many areas during the summer of 2021-2022, with large numbers of cloudy days, lower levels of evaporation, and extended periods of leaf wetness. Observations in Indonesia suggest that the development of scab caused by *E. necatrix*, similar to that of other *elsinoe* diseases, is strongly dependent on relative humidity and leaf wetness (Li *et al.*, 2021; Pham *et al.*, 2021).

It is as yet unknown what the economic impact of the disease caused by *E. masingae* may be. However, based on observations in some plantations, growth losses can be expected, particularly in cases of repeated outbreaks of infection. Fortunately, as observed in Indonesia (Pham *et al.*, 2021), considerable variation in susceptibility has been observed between different *Eucalyptus* genotypes in South Africa. This, together with the avoidance of sites having high moisture levels, may allow successful management of the disease.

Conclusion

Elsinoe masingae is the second species of *Elsinoe* recently reported to cause a serious scab and shoot malformation disease of plantation-grown *Eucalyptus* species. Prior to the description of *E. necatrix* from Indonesia, *Elsinoe* species were not known as important pathogens of *Eucalyptus*. The disease in South Africa is already wide-spread and based on disease severity in some plantations, its impact could be significant. Studies to understand the possible origin and genetic diversity of *E. masingae* are now required to inform selection of disease tolerant planting material. Together with site matching this should reduce economic losses due to *E. masingae*.

Funding

This work was supported by the Tree Protection Cooperative Programme (TCP) of the Forestry and Agricultural Biotechnology Institute (FABI), the University of Pretoria (South Africa) and the National Research Foundation (NRF), South Africa.

Acknowledgements

Mr Sandile Masinga is thanked for bringing the disease described in this study to our attention.

Conflict of interest statement

None declared.

Data availability statement

The data underlying this article are available in the article and in its online supplementary material. Sequence and other data is available from the respective data repositories as indicated in the article.

References

- Bonello, P., Carnegie, A.J. and Ormsby, M. 2022 Editorial: Forest Biosecurity Systems and Processes: A global perspective. *Front. For. Glob. Change* **5**, 1-3.
- Branco, M., Bockerhoff, E.G., Castagnyrol, B., Orazio, C. and Jactel, H. 2015 Host range expansion of native insects to exotic trees increases with area of introduction and the presence of congeneric native trees. *J. Appl. Ecol.* **52**, 69–77.
- Cheewangkoon, R., Groenewald, J.Z., Summerell, B.A., Hyde, K.D., To-anun, C. and Crous, P.W. 2009. Myrtaceae, a cache of fungal biodiversity. *Persoonia* **23**, 55–85.
- Crous, P.W., Wingfield, M.J., Burgess, T.I., Hardy, G.E.St.J., Crane, C., Barrett, S., Cano-Lira, J.F., Le Roux, J.J., Thangavel, R., Guarro, J., Stchigel, A.M., Martin, M.P., Alfred, D.S., Barber, P.A., Barreto, R.W., Baseia, I.G., Cano-Canals, J., Cheewangkoon, R., Ferreira, R.J., Gené, J., Lechat, C., Moreno, G., Roets, F., Shivas, R.G., Sousa, J.O., Tan, Y.P., Wiederhold, N.P., Abell, S.E., Accioly, T., Albizu, J.L., Alves, J.L., Antonioli, Z.I., Aplin, N., Araújo, J., Arzanlou, M., Bezerra, J.D.P., Bouchara, J.-P., Carlavilla, J.R., Castillo, A., Castroagudín, V.L., Ceresini, P.C., Claridge, G.F., Coelho, G., Coimbra, V.R.M., Costa, L.A., Da Cunha, K.C., Da Silva, S.S., Daniel, R., De Beer, Z.W., Dueñas, M., Edwards, J., Enwistle, P., Fiuza, P.O., Fournier, J., García, D., Gibertoni, T.B., Giraud, S., Guevara-Suarez, M., Gusmão, L.F.P., Haituk, S., Heykoop, M., Hirooka, Y., Hofmann, T.A., Houbraeken, J., Hughes, D.P., Kautmanová, I., Koppel, O., Koukol, O., Larsson, E., Latha, K.P.D., Lee, D.H., Lisboa, D.O., Lisboa, W.S., López-Villalba, Á., Maciel, J.L.N., Manimohan, P., Manjón, J.L., Marincowitz, S., Marney, T.S., Meijer, M., Miller, A.N., Olarija, I., Paiva, L.M., Piepenbring, M., Poveda-Molero, J.C., Raj, K.N.A., Raja, H.A., Rougeron, A., Salcedo, I., Samadi, R., Santos, T.A.B., Scarlett, K., Seifert, K.A., Shuttleworth, L.A., Silva, G.A., Silva, M., Siqueira, J.P.Z., Souza-Motta, C.M., Stephenson, S.L., Sutton, D.A., Tamakeaw, N., Telleria, M.T., Valenzuela-Lopez, N., Viljoen, A., Visagie, C.M., Vizzini, A., Wartcho, F., Wingfield, B.D., Yurchenko, E., Zamora, J.C. and Groenewald, J. Z. 2016. Fungal Planet description sheets: 469-557. *Persoonia* **36**, 218-403.
- Crous, P.W., Wingfield, M.J., Cheewangkoon, R., Carnegie, A.J., Burgess, T.I., Summerell, B.A., Edwards, J., Taylors, P.W.J. and Groenewald, J.Z. 2019 Foliar pathogens of eucalypts. *Stud. Mycol.* **94**, 125–298.
- Dittrich-Schröder, G., Wingfield, M.J., Hurley, B.P. and Slippers, B. 2012 Diversity in *Eucalyptus* susceptibility to the gall-forming wasp *Leptocybe invasa*. *Agr. Forest Entomol.* **14**, 429-427.
- Doidge, E.M. 1950 The South African fungi and lichens. *Bothalia* **5**, 1-1094.

- Fan, X.L., Barreto, R.W., Groenewald, J.Z., Bezerra, J.D.P., Pereira, O.L., Cheewangkoon, R., Mostert, L., Tian, C.M. and Crous, P.W. 2017 Phylogeny and taxonomy of the scab and spot anthracnose fungus *Elsinoë* (Myriangiales, Dothideomycetes). *Stud. Mycol.* **87**, 1–41.
- Gardes, M. and Bruns, T.D. 1993 ITS primers with enhanced specificity for basidiomycetes—application to the identification of mycorrhizae and rusts. *Mol. Ecol.* **2**, 113–118.
- Greyling, I., Wingfield, M.J., Coetzee, M.P.A., Marincowitz S. and Roux, J. 2016. The *Eucalyptus* shoot and leaf pathogen *Teratosphaeria destructans* recorded in South Africa. *South. For.* **78**, 123–129.
- Hyun, J.W., Yi, S.H., MacKenzie, S.J., Timmer, L.W., Kim, K.S., Kang, S.K., Kwon, H.M. and Lim, H.C. 2009 Pathotypes and genetic relationship of worldwide collections of *Elsinoë* spp. causing scab diseases of citrus. *Phytopathology* **99**, 721–728.
- Katoh, K. and Standley, D.M. 2013 MAFFT multiple sequence alignment software version 7: improvements in performance and usability. *Mol. Biol. Evol.* **30**, 772–780.
- Kotzé, J.J. 1935 *Forest fungi: The position in South Africa*. In: Papers and statements on exotics, 4th British Empire Forestry Conference. Government Printer, Pretoria, South Africa.
- Kumar, S., Stecher, G. and Tamura, K. 2016 MEGA7: Molecular Evolutionary Genetics Analysis version 7.0 for bigger datasets. *Mol. Biol. Evol.* **33**, 1870–1874.
- Li, Z., Dos Santos, R.F., Gao, L., Chang, P. and Wang, X. 2021. Current status and future prospects of grapevine anthracnose caused by *Elsinoë ampelina*: An important disease in humid grape-growing regions. *Mol. Plant Pathol.* **22**, 899–910.
- Liao, H.L. and Chung, K.R. 2008 Cellular toxicity of elsinochrome phytotoxins produced by the pathogenic fungus, *Elsinoe fawcettii* causing citrus scab. *New Phytol.* **177**, 239–250.
- Liu, Y.J., Whelen, S. and Hall, B.D. 1999 Phylogenetic relationships among ascomycetes: evidence from an RNA polymerase II subunit. *Mol. Biol. Evol.* **16**, 1799–1808.
- Marin-Felix, Y., Hernández-Restrepo, M., Iturrieta-González, I., García, D., Gené, J., Groenewald, J.Z., Cai, L., Chen, Q., Quaedvlieg, W., Schumacher, R.K., Taylor, P.W.J., Ambers, C., Bonthondi, G., Edwards, J., Krueger-Hadfield, S.A., Luangsa-ard, J.J., Morton, L., Moslemi, A., Sandoval-Denis, M., Tan, Y.P., Thangavel, R., Vaghefi, N., Cheewangkoon, R. and Crous, P.W. 2019 Genera of phytopathogenic fungi: GOPHY 3. *Stud. Mycol.* **94**, 1–124.
- Morris, A.R. 2022. Changing use of species and hybrids in South African forest plantations. *South. For.* **84**, 01–13.
- Oberholzer, F. 2021 *South African Forestry and forest products industry 2019*. Forestry South Africa. (<https://www.forestry.co.za/statistical-data/>).
- Pham, N.Q., Marincowitz, S., Solis, M., Duong, T.A., Wingfield, B.D., Barnes, I., Slippers, B., Muro Abad, J.I., Durán, A. and Wingfield, M.J. 2021 Eucalyptus scab and shoot malformation: A new and serious foliar disease of *Eucalyptus* caused by *Elsinoë necatrix* sp. nov. *Plant Pathol.* **70**, 1230–1242.
- Posada, D. 2008 jModelTest: phylogenetic model averaging. *Mol. Biol. Evol.* **25**, 1253–1256.
- Poynton, R.J. 1979. *Tree Planting in Southern Africa. Volume 2 The Eucalypts*. Department of Forestry, Republic of South Africa, 882 pp.
- Rambaut, A. 2010 *FigTree v1.3.1*. Institute of Evolutionary Biology, University of Edinburgh, Edinburgh. <http://tree.bio.ed.ac.uk/software/figtree/>
- Ramsfield, T.D., Bentz, B.J., Faccoli, M., Jactel, H. and Brockerhoff, E.G. 2016. Forest health in a changing world: effects of globalization and climate change on forest insect and pathogen impacts. *Forestry (Lond)* **89**, 245–252.
- Rayner RW. 1970. *A mycological colour chart*. Commonwealth Mycological Institute, Kew, Surrey, and British Mycological Society. 37 p.

- Rehner, S.A. and Samuels, G.J. 1994 Taxonomy and phylogeny of *Gliocladium* analysed from nuclear large subunit ribosomal DNA sequences. *Mycol. Res.* **98**, 625–634.
- Ronquist, F., Teslenko, M., van der Mark, P., Ayres, D.L., Darling, A., Höhna, S., Larget, B., Liu, L., Suchard, M.A., and Huelsenbeck, J.P. 2012 MrBayes 3.2: efficient Bayesian phylogenetic inference and model choice across a large model space. *Syst. Biol.* **61**, 539–542.
- Roux, J., Hurley, B.P. and Wingfield, M.J. 2012 *Diseases and pests of Eucalyptus, Pines and Wattle*. In South African Forestry Handbook, vol 1 (5th edition). B.V. Bredenkamp and S.J. Upfold (eds). South African Institute for Forestry, pp. 303-336.
- Roux, J., Wingfield, M.J., Fourie, A., Noeth, K. and Barnes, I. 2020 Ceratocystis wilt on *Eucalyptus*: first record from South Africa. *South. For.* **82**:24-31.
- Slippers, B., Hurley, B.P. and Allison, J.D. 2020a. Harnessing the potential of Precision Pest Management in plantation forests. *South. For.* **82**, 197-201.
- Slippers, B., Visser, M. and Roux, J. 2020b. Why it's so critical to continuously monitor and manage plant diseases. *The Conversation* https://theconversation.com/why-its-so-critical-to-continuously-monitor-and-manage-plant-diseases-139423#comment_2251101.
- Stamatakis, A. 2014 RAxML version 8: a tool for phylogenetic analysis and post-analysis of large phylogenies. *Bioinformatics* **30**, 1312–1313.
- Summerell, B.A., Groenewald, J.Z., Carnegie, A.J. and Summerbell, R. 2006. *Eucalyptus* microfungi known from culture. 2. *Alysiidiella*, *Fusculina* and *Phlogicylindrium* genera nova, with notes on some other poorly known taxa. *Fungal Divers.* **23**, 323–350.
- Sung, G.H., Sung, J.M., Hywel-Jones, N.L. and Spatafora, J.W. 2007. A multi-gene phylogeny of Clavicipitaceae (Ascomycota Fungi): identification of localized incongruence using a combinational bootstrap approach. *Mol. Phylogenet. Evol.* **44**, 1204–1223.
- Taylor, J.W., Jacobson, D.J., Kroken, S., Kasuga, T., Geiser, D.M., Hibbett, D.S. and Fisher, M.C. 2000. Phylogenetic species recognition and species concepts in fungi. *Fungal Genet. Biol.* **31**, pp.21-32.
- Van Heerden, S.W., Amerson, H.V., Preisig, O., Wingfield, B.D. and Wingfield, M.J. 2005 Relative pathogenicity of *Cryphonectria cubensis* on *Eucalyptus* clones differing in their resistance to *C. cubensis*. *Plant Dis.* **89**, 659-662.
- Vilgalys, R. and Hester, M. 1990 Rapid genetic identification and mapping of enzymatically amplified ribosomal DNA from several *Cryptococcus* species. *J. Bacteriol.* **172**, 4238–4246.
- White, T.J., Bruns, T., Lee, S. and Taylor, J.W. 1990 *Amplification and direct sequencing of fungal ribosomal RNA genes for phylogenetics*. In: Innis MA, Gelfand DH, Sninsky JJ, White TJ (eds) PCR protocols: a guide to methods and applications. San Diego, CA: Academic, pp 315–322.
- Wingfield, M.J., and Knox-Davies, P.S. 1980 Observations on diseases in pine and *Eucalyptus* plantations in South Africa. *Phytophylactica* **12**, 57-63
- Wingfield, M.J., Slippers, B., Hurley, B.P., Coutinho, T.A., Wingfield, B.D. and Roux J. 2008 Eucalypt pests and diseases: growing threats to plantation productivity. *South. For.* **70**, 139-144.
- Wingfield, M.J., Brockerhoff, E.G., Wingfield, B.D. and Slippers, B. 2015. Planted forest health: The need for a global strategy. *Science* **349**, 832-836.